Weak trimerization in the frustrated two-dimensional triangular Heisenberg antiferromagnet math xmlns="http://www.w3.org/1998/Math/MathML">msub>mi mathvariant="normal">Lu/mi>mi>y/mi>/msub>msub>mi mathvariant="normal">Y/mi>mrow>mn>1/mn>mo>−/mo >mi>y/mi>/mrow>/msub>msub>mi mathvariant="normal">MnO/mi>mn>3/mn>/msub>/math >

S. Yano, Chin-Wei Wang, Jason S. Gardner, Wei-Tin Chen, Kazuki Iida, R. A. Mole, and Despina Louca

Phys. Rev. B **107**, 214407 — Published 2 June 2023

DOI: 10.1103/PhysRevB.107.214407

A Weak Trimerization in the Frustrated 2D Triangular Heisenberg Antiferromagnet $Lu_yY_{1-y}MnO_3$

S. Yano, Chin-wei Wang,[1] Jason S. Gardner,[2] Wei-Tin Chen,[3,4] Kazuki Iida,[5] R. A. Mole,[6] and Despina Louca[7]

[1]*National Synchrotron Radiation Research Center, Neutron Group, Hsinchu 30077, Taiwan.*
[2]*Material Science and Technology Division, Oak Ridge National Laboratory, Oak Ridge, Tennessee 37831, USA*
[3]*Center for Condensed Matter Sciences and Center of Atomic Initiative for New Materials, National Taiwan University, Taipei 10617, Taiwan*
[4]*Taiwan Consortium of Emergent Crystalline Materials, National Science and Technology Council, Taipei 10622, Taiwan*
[5]*Neutron Science and Technology Center, Comprehensive Research Organization for Science and Society (CROSS), Tokai, Ibaraki 319-1106, Japan*
[6]*Australian Nuclear Science and Technology Organisation, Lucas Heights, New South Wales 2232, Australia*
[7]*University of Virginia, Department of Physics,Charlottesville, Virginia 22904, USA.*

(Dated: May 11, 2023)

To understand 2D Triangular Heisenberg Antiferromagnetic system, we investigated the magnetic structures and the dynamics of $Lu_yY_{1-y}MnO_3$ in detail. The substitutions are adjusted to the Mn atomic position close to $x_{Mn} = \frac{1}{3}$. The neutron powder diffraction data claims that the magnetic structure of $Lu_yY_{1-y}MnO_3$ is described as a mixture of Γ_3 ($P6'_3cm'$) and Γ_4 ($P6'_3c'm$) at the x_{Mn} position for $y = 0.15$, 0.30, and 0.45. The ratio of Γ_3 and Γ_4 depends on temperature and composition and the fraction of Γ_3 increases upon cooling while no clear trimerization was observed at the x_{Mn} position. We estimated exchange parameters from the analysis of the low energy part of the spin waves. The results showed a weak trimerization effect on cooling because the nearest neighbour exchange interaction is slightly enhanced. The temperature dependence of the spin wave dispersion around the Γ point shows that the spin gap closes with increasing temperature because the exchange interactions in the nearest Mn-Mn neighbour become smaller. Gap-less diffusive magnetic excitation from a Mn triangular lattice has been observed in a wide range in Q and E space of $Lu_yY_{1-y}MnO_3$. We found that $Lu_{0.7}Y_{0.3}MnO_3$ could be an ideal case to investigate trimerization, frustrated magnetism, and magnetoelastic coupling often observed in the 2D-THA systems.

PACS numbers:

INTRODUCTION

A two-dimensional triangular lattice Heisenberg antiferromagnet (2D-THA) is one of the simplest examples of a geometrically frustrated antiferromagnet. A novel spin state originates from low dimensionality and competing magnetic interactions. One of the earliest examples of multiferroic materials is the hexagonal RMnO$_3$ family (R is a rare earth ion with a small radius such as Y, Lu, Ho, and Yb) [1]. Given that RMnO$_3$ is a frustrated magnetic system with magneto-elastic coupling, trimerization is expected to stabilize the magnetic structure. The coupled trimerization distortion has been reported to occur in the hexagonal plane in $YMnO_3$ and $LuMnO_3$ where Y and Lu are non-magnetic atoms. In the former the lattice expands, while in the latter it contracts [2].

We report on the magnetic properties of $Lu_yY_{1-y}MnO_3$. The parent compounds $YMnO_3$ and $LuMnO_3$ has been investigated for decades. The crystal structure of (Y, Lu)MnO$_3$ transforms to the $P63cm$ symmetry upon entering the ferroelectric phase at high temperatures ($\sim$ 900 K). The antiferromagnetic phase appears below ($\sim$ 90 K) [3]. The symmetry could be lower upon entering the magnetic phase based on local structure analysis [4]. The magnetic excitations of $Lu_yY_{1-y}MnO_3$ has been fully investigated for $YMnO_3$ [5–8], $LuMnO_3$ [9], and $Lu_{0.3}Y_{0.7}MnO_3$ [10] by linear spin wave theory. Magnon-phonon coupling has been introduced to improve the model of the magnetic excitations for this system. The clear deviation of the dispersion predicted by linear spin wave theory reveals magneto-elastic excitations with spontaneous decay in $LuMnO_3$, $Lu_{0.5}Y_{0.5}MnO_3$, and $YMnO_3$ [11, 12]. The magnon dispersion can be explained by using the model $J_1 = J_2$ by introducing α, a dimensionless exchange-striction coefficient. DFT calculations show that there is 10-20 percent difference in J_1 and J_2. The magneto-elastic coupling model of super-exchange qualitatively reproduces the experimental observation on $YMnO_3$ [13]. The phonon part of the magneto-elastic excitation in $YMnO_3$ has been examined using inelastic X-ray scattering (IXS). Their theoretical model based on a super exchange striction mechanism can explain the magnon phonon coupling and provides the effect of magnon-phonon coupling for individual modes[13]. Another result from $Lu_{0.3}Y_{0.7}MnO_3$ [10] provide strong evidence that the magnitude of magnetoelectric coupling is linked to the strength of the trimerization distortion, suggesting the Mn trimerization is responsible for the magnetoelectric effect in $Lu_yY_{1-y}MnO_3$. However,

these excitations and determined parameters should be studied carefully since these parameters should be delicately balanced. In this paper, we carefully chose the compositions and temperatures to capture slight changes near the perfect Mn triangular lattice so we can monitor the parameter change carefully to understand the 2D-THA system better.

Here, we focus on $Lu_yY_{1-y}MnO_3$ (y =0.15, 0.30, and 0.45) for the following reasons. Neutron inelastic scattering experiments on RMnO$_3$ (R = Ho, Yb, Sc, and Y) claimed that the $x_{Mn} = 1/3$ is the key to determining the coupling between Mn triangular planes [14] shown in Figure 1 (a) and (b). Upon substituting nonmagnetic Lu and Y, the Mn atomic positions have been shown to change. For example, the Mn atomic position (x_{Mn}, 0, 0) in $LuMnO_3$ is $x_{Mn} = 0.331$, that of $YMnO_3$ is $x_{Mn} = 0.340$. While for $Lu_{0.3}Y_{0.7}MnO_3$, the Mn atomic position is $x_{Mn} = 1/3$ [3]. The atomic displacement triggered by the x_{Mn} position change may cause the multiferroic properties of hexagonal manganites via strong spin-lattice coupling. High-resolution neutron and synchrotron powder diffraction experiments have shown that the Mn positions have shifted away from $x_{Mn} = 1/3$ in $LuMnO_3$, $YMnO_3$, and $Lu_{0.5}Y_{0.5}MnO_3$ at their T_Ns. [33]. The spin reorientation transition observed in $HoMnO_3$ presents a way to test this prediction: above T_{SR} where the structure is Γ_4, one would expect to observe $x_{Mn} < 1/3$, whilst below T_{SR} the structure is Γ_1, implying $x_{Mn} > 1/3$. Neutron diffraction measurements appear to support this hypothesis, albeit with sizeable uncertainties [14]. The atomic position of $YMnO_3$ of $x_{Mn} > 1/3$ and that of $LuMnO_3$ of $x_{Mn} < 1/3$ are shown in figure 1 (a) and (b). The two different exchange parameters J_1 and J_2 are due to the position of Mn that is not at $x_{Mn} = 1/3$. For $x_{Mn} > 1/3$, 4 J_1 and 2 J_2 are in the plane. For $x_{Mn} < 1/3$, 2 J_1 and 4 J_2 are in the plane. Subtle changes in the exchange parameters can be captured when we use the sample close to a perfect triangular lattice. The $Lu_yY_{1-y}MnO_3$ (y =0.15, 0.30, and 0.45) is the ideal compound to study this effect further because the x_{Mn} is very close to the 1/3.

In addition, the magnetic structure of the family has been shown to be highly dependent on the composition with structures varying from Γ_3 ($P6'_3cm'$) with a small fraction of Γ_4 ($P6'_3c'm$) in $YMnO_3$ to the Γ_4 with a small fraction of Γ_3 in $LuMnO_3$[3] as shown in the figure 1 (c). The small difference in the crystal structure could affect the magnetic structure of $Lu_yY_{1-y}MnO_3$. So that the $Lu_yY_{1-y}MnO_3$ (y =0.15, 0.30, and 0.45) are a good playground to investigate their crystal structures, magnetic structures, and trimerization. The first principal electronic structure calculations in local density approximations indicated that the ground states of $YMnO_3$ and $LuMnO_3$ are in agreement with the experiment. All states are located in a narrow energy range, which is expected for a frustrated magnetic system [2]. The single-ion anisotropy is the origin of the different magnetic structures of $YMnO_3$ and $LuMnO_3$. So we believe that precise crystal and magnetic structures are critical to understanding the physical properties of this system. Especially, the exchange parameters should be extracted from spin waves with high energy resolution by using precise structural parameters.

Finally, the diffuse scattering has been observed for $YMnO_3$ and $LuMnO_3$ in both powders and single crystals experiments [9, 17–19]. These studies indicate diffuse scattering extends into the inelastic scattering. This phenomena has been observed in many of the 2D-THA materials such as $CuCrO_2$ [20] and $Lu_{0.5}Sc_{0.5}FeO_3$ [21, 22]. This effect is not limited to 2D-THA materials and is typically observed in so-called frustrated magnets including candidates of a quantum spin liquid state. For example, ZnV_2O_4 [23],$ZnCr_2O_4$ [24], $MgCr_2O_4$ [25], herbertmithite [26], and $YbMgGaO_4$ [27], and $Li_2AMo_3O_8$ (A=In, Sc) [28] show similar diffusive scattering. However, it has never been systematically investigated. More recent neutron scattering experiment on the single crystal of $YMnO_3$ [29] observed diffuse scattering above the T_N = 71K as well. The constant energy maps with $\hbar\omega = 1.0 \pm 0.2$ meV show a broad peak of bright intensity resides at Γ' point, such as (100), (200) but not at the Γ point like (110). The signal is strongest for small Q as expected due to the magnetic form factor as we see in these three samples. The diffuse scattering of the single crystal of $YMnO_3$ has been discussed as the critical spin fluctuation existing in a vastly extended critical range due to frustration. The paper suggested that the more precise definition of classical spin liquid state due to geometrical frustration is worth exploring.

Here, we have studied polycrystalline and single crystal samples of $Lu_yY_{1-y}MnO_3$, here Lu and Y are nonmagnetic. The structural analyses show no obvious trimerization in the composition of y = 0.15, 0.30 and 0.45. The symmetry of the magnetic structure is described by linear combinations of Γ_3 and Γ_4 which is equivalent to Γ_6 reported in polarized neutron scattering techniques [16]. The magnetic structure can be described by an increasing fraction of Γ_3 indicating $Lu_yY_{1-y}MnO_3$ favours Γ_3 over Γ_4. The Lu substitution increases the fraction of Γ_4. Inelastic neutron scattering experiments captured a weak trimerization on the exchange coupling of Mn-Mn upon cooling the system. The spin wave gap of $Lu_{0.3}Y_{0.7}MnO_3$ is about five times smaller than that of $LuMnO_3$ and $YMnO_3$ due to in-plane anisotropy being D_2 one order of magnitude smaller. While exchange parameters J_1, J_2, and out of plane anisotropy D_1 are of the same order. The inter layer coupling is weak so that two-dimensional spin fluctuations remain. We show the single crystal of $Lu_{0.3}Y_{0.7}MnO_3$ could be a suitable candidate to investigate the diffusive behaviour above T_N on the 2D-THAs and other frustrated magnets.

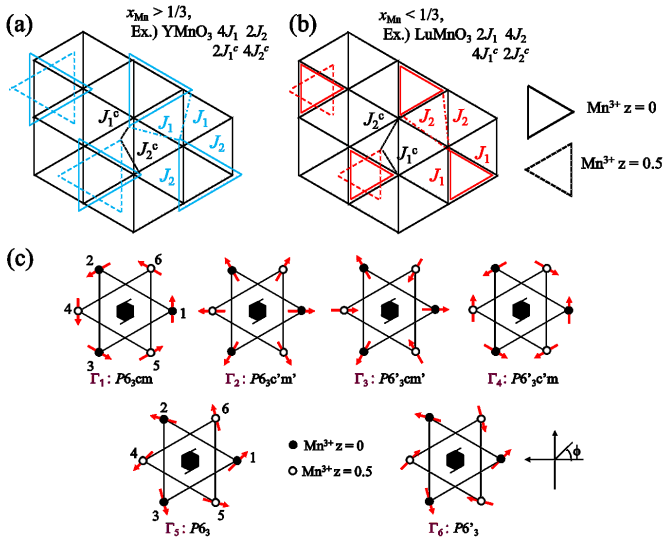

FIG. 1: (a) and (b) The exchange interaction between Mn-Mn (x_{Mn}, 0, 0) site. The $x_{Mn} = 1/3$ is the key to define J_1 and J_2. (c) The six types of 120 degrees antiferromagnetic structures could be realized under the $P6_3cm$.

Experiment

Polycrystalline samples of $Lu_yY_{1-y}MnO_3$ were prepared by solid state reaction [3]. A single crystal of $Lu_{0.3}Y_{0.7}MnO_3$ sized 4mm ϕ*35 mm (approx. 4g) was prepared by floating zone method [10]. Neutron diffraction data were collected at the high-intensity neutron diffractometer WOMBAT [30] at the Australian Centre for Neutron Scattering (ACNS) in the Australian Nuclear Science and Technology Organisation (ANSTO). Inelastic neutron scattering studies on the single crystal sample were performed with the cold triple-axis spectrometer SIKA at ACNS, ANSTO [31]. Data were collected with two different fixed final energies, with $E_f = 5.0$ meV and 3.0 meV. The energy resolution for these two configurations is 0.15 meV and 0.04 meV respectively. A cooled Be-filter was placed in the scattered beam to filter higher-order neutrons. Further inelastic neutron scattering data were acquired using the cold-neutron time-of-flight spectrometer PELICAN[32]. 19.0 grams ($y = 0.15$), 26.4 grams ($y = 0.30$), and 16.8 grams ($y = 0.45$) of samples were held in an annular aluminium can to minimise multiple scattering. Data was collected with E_i=3.69 meV.

Crystal and Magnetic structures of $Lu_yY_{1-y}MnO_3$

A large number of structural analyses on the $RMnO_3$ have been already performed and the systematic study of the structure of $Lu_yY_{1-y}MnO_3$ has been performed by several groups [3, 33, 34]. One of the interesting phenomena reported is the temperature dependence of the atomic position of Mn. Their positions shift away from the ideal value of $x_{Mn} = 1/3$ when the system goes into the magnetically ordered state [33]. The Mn atomic position of $x_{Mn} = 1/3$ is the key to determining the coupling between Mn triangular planes [14].

We have performed the crystal and magnetic structural analyses of three compositions of $Lu_yY_{1-y}MnO_3$ with $y = 0.15$, 0.30 and 0.45. The system remains in the space group of $P6_3cm$ (No. 185) above and below the ordering transition and this was used to fit powder diffraction data. The magnetic ordering is observed at around $T_N = 80K$ which is consistent with previous studies 2(a)). The magnetic structure of $Lu_yY_{1-y}MnO_3$, for all three compositions are described as one of two sets of linear combinations of irreducible representations $C_1\Gamma_1 + C_2\Gamma_2$ or $C_3\Gamma_3 + C_4\Gamma_4$. We found that both sets equally well fit the data set. We should note that these irreducible representations are analogous to the following Shubnikov groups, Γ_1 ($P6_3cm$), Γ_2($P6_3c'm'$), Γ_3 ($P6'_3cm'$), and Γ_4 ($P6'_3c'm$) summarized in Table I. Γ_1 and Γ_3 cannot be distinguished by powder diffraction, which is also true for Γ_2 and Γ_4. The magnetic component of the c axis is also excluded from the analysis. So the magnetic structural analysis of a polycrystalline sample is unable to determine which magnetic structure with these 120 degrees configurations is right.

We picked the combination of $C_3\Gamma_3 + C_4\Gamma_4$ for the magnetic structure model for $Lu_yY_{1-y}MnO_3$, that explains the powder diffraction pattern well. The fraction of Γ_4 grows by increasing Lu content. The Mn positions (x_{Mn}, 0, 0) are close to $x_{Mn} = 0.333$ for $y = 0.15$ and 0.30. While for $y = 0.45$ the position is slightly below $x_{Mn} = 0.333$. There is a reduction in x_{Mn} at T_N observed in all three compounds unlike $YMnO_3$, $LuMnO_3$, and $Lu_{0.5}Y_{0.5}MnO_3$ [33]. Interestingly, the fraction of Γ_3 keeps growing for all three compositions upon cooling. On the other hand, that of Γ_4 saturates or even decreases by cooling the sample. Consequently, ϕ keeps decreasing while cooling these systems which indicates $Lu_yY_{1-y}MnO_3$ favours Γ_3 over Γ_4 as the ground state. The x_{Mn} positions of all three compositions are close to 1/3, however, no sudden change was observed in temperature below 100 K (Figure 2(b)). The Mn atoms form close to a perfect triangular lattice upon substituting (Y, Lu). There is no spin reorientation observed like in $HoMnO_3$ or $ScMnO_3$ [14].

As far as the neutron powder diffraction data is concerned, the combination of $C_1\Gamma_1 + C_2\Gamma_2$ or $C_3\Gamma_3 + C_4\Gamma_4$ gives the same R factors. So these two structures fit the experimental data equally well. The Second harmonic generation result claims the symmetry of the magnetic structure of $YMnO_3$ is Γ_3 ($P6'_3cm'$) [15], on the other hand, the polarized neutron scattering experiment shows that of $YMnO_3$ is Γ_6 ($P6'_3$) [16]. We at-

	Γ_1	Γ_2	Γ_3	Γ_4
Mn (6*c*)	$P6_3cm$	$P6_3c'm'$	$P6'_3cm'$	$P6'_3c'm$
(x, y, z)	(u, 2u, 0)	(u, 0, v)	(u, 0, v)	(u, 2u, 0)
$(-x, -y, z+\frac{1}{2})$	(-u, -2u, 0)	(-u, 0, v)	(u, 0, -v)	(u, 2u, 0)
$(-y, x-y, z)$	(-2u, -u, 0)	(0, u, v)	(0, u, v)	(-2u, -u, 0)
$(y, -x+y, z+\frac{1}{2})$	(2u, u, 0)	(0, -u, v)	(0, u, -v)	(-2u, -u, 0)
$(-x+y, -x, z)$	(u, -u, 0)	(-u, -u, v)	(-u, -u, v)	(u,-u,0)
$(x-y, x, z+\frac{1}{2})$	(-u, u, 0)	(u, u, v)	(-u, -u, v)	(u, -u, 0)

TABLE I: The four Irreducible representations of the small group obtained from the space group $P6_3cm$ for $\vec{k} = (0,0,0)$ and the corresponding basis vectors. These u and v are coefficients, such as (u, 2u, 0) = u*(1, 0 0) + 2u*(0, 1, 0), (u, 0, v)=u*(1, 0 ,0)+v*(0, 0, 1)), and so on.

tempted to solve the magnetic structure using Γ_6 only however, this did not really describe the observed data. In fact, the linear combination of Γ_3 and Γ_4 can create the magnetic structure which has the $P6'_3$ symmetry. So, we employed the combination by following the argument by Brown and Chatterji [16]. These magnetic structures of $Lu_{0.15}Y_{0.85}MnO_3$ with $\phi = 8.6$ degree and $Lu_{0.30}Y_{0.70}MnO_3$ $\phi = 13.7$ degree at $T = 3.7$ K are consistent with polarized neutron scattering result of $YMnO_3$ which is Γ_6 ($P6'_3$) with $\phi = 11$ degrees at $T = 4$ K [16]. From the previous reports, $YMnO_3$ and $LuMnO_3$ form different magnetic structures in the ground state. The main reason why $YMnO_3$ and $LuMnO_3$ have different magnetic structures is related to the single-ion anisotropy with a corresponding distortion of the Mn triangles based on their electric low-energy model for Mn 3*d* bands for $YMnO_3$ and $LuMnO_3$[2]. Either way, there is no clear trimerization of Mn lattice at $Lu_yY_{1-y}MnO_3$ (y=0.15, 0.30, and 0,45) from our observation.

Spin waves dispersion in $Lu_{0.3}Y_{0.7}MnO_3$

The magnetic excitations of a single crystal sample of $Lu_{0.3}Y_{0.7}MnO_3$ have been investigated in detail using the cold triple-axis spectrometer SIKA. At $y = 0.30$, it should be close to the perfect triangular lattice compared to $YMnO_3$ and $LuMnO_3$ as we have shown in the previous section.

We performed a detailed investigation of the low-energy modes with a high-energy resolution to estimate exchange parameters as precisely as possible based on the parameters we optimized in the last section. We also report the spin wave dispersion around the Γ point at lower energy ($\sim$ 8 meV) where the magnon-phonon coupling is supposed to be weak [13], thus linear spin wave theory is applicable. Based on previous research [5, 10], there are four branches $\Delta_{11}, \Delta_{12}, \Delta_2$ and Δ_3. The Δ_2 and Δ_3 are approximately degenerate around the (100) with an energy of 6 meV. The Δ_{11} and Δ_{12} are also degenerate

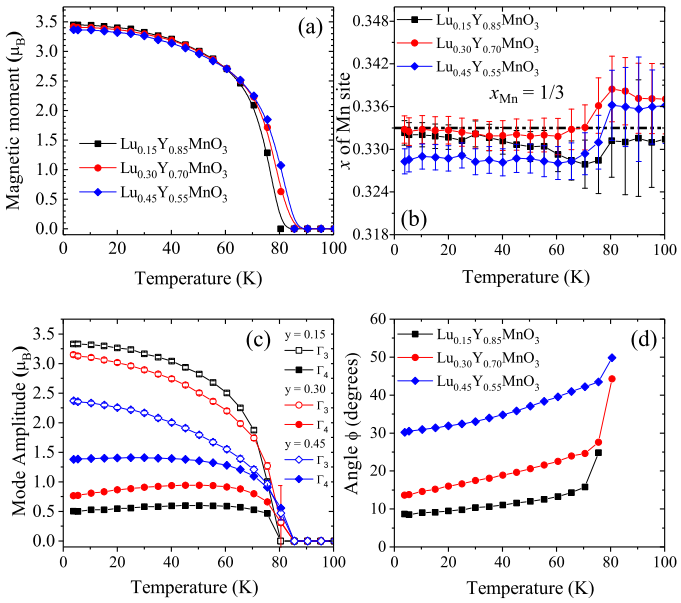

FIG. 2: (a) Temperature dependence of magnetic moment of Mn sites. (b) Temperature dependence of (x_{Mn}, 0, 0) site. (c) The determined magnetic structure of $Lu_yY_{1-y}MnO_3$ (d) The temperature dependence of the angle ϕ with Γ_3. At $\phi =$ keep decreasing the angle so the ratio of Γ_3 increases with the $C_3\Gamma_3 + C_4\Gamma_4$

and the doublet shows a gap at the Γ point. This gap is an order of magnitude smaller than that reported for $YMnO_3$ and $LuMnO_3$ [5, 9, 10] as shown in Figure 3. Figure 3 shows that spin wave dispersion at 1.5, 35, and 70 K (near T_N). Intensities have been normalized to the incident neutron flux and correspond to around 3 minutes per point. The spin wave measurement shows that the slight change in the magnetic structure with changing temperature does not significantly affect the spin wave dispersion, however, it does slightly affect the scattering intensities. The dispersion softens while the temperature of the sample increases. Just below T_N, the branches of Δ_2 and Δ_3 shift to low energy while the gap of the Δ_{11} and Δ_{12} become zero within the energy resolution of the instrumental configuration.

Analysis of spin waves

A number of analysis on spin dynamics on $Lu_yY_{1-y}MnO_3$ have been performed [5–7, 9, 10, 12, 35, 36]. The results are summarized in Table II. These analyses are made based on the Hamiltonian below. A quantitative comparison between $YMnO_3$, $Lu_{0.3}Y_{0.7}MnO_3$, and $LuMnO_3$ have been made. Many of them analyzed spin wave dispersion by using linear spin wave theory.

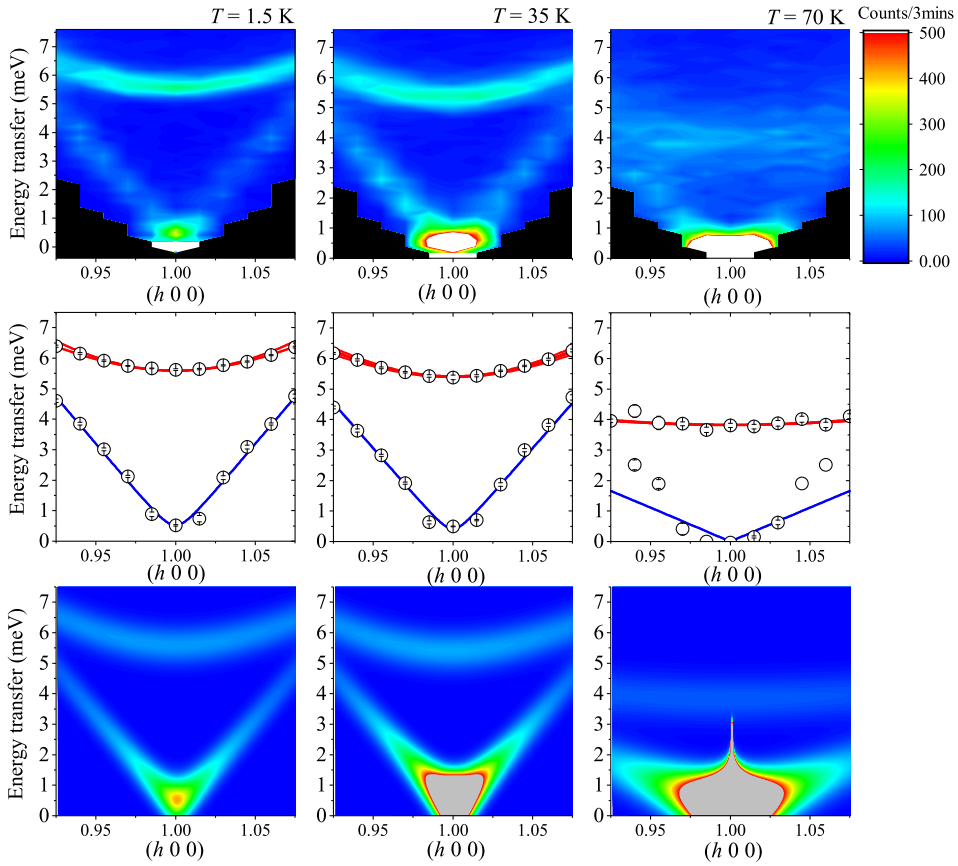

FIG. 3: Color map of the scattering intensities observed in the (h 0 0) h = 0.925 - 1.075 at 1.5K, 35 K and 70 K. 2nd row) The theoretically calculated the dispersion within the combination of $C_3\Gamma_3 + C_4\Gamma_4$ and experimental data at the same q values, 3rd row) The theoretically calculated intensities with in the combination of $C_3\Gamma_3 + C_4\Gamma_4$ of the dispersion at the same q values.

$$H = \sum_{intra} J_i \mathbf{S}_i \cdot \mathbf{S}_j + \sum_{inter} J_i^c \mathbf{S}_i \cdot \mathbf{S}_j + H_{aniso} \qquad (1)$$

The two intra-plane exchange parameters J_1 and J_2 arise from the difference in the position of Mn away from the ideal $x_{Mn} = 1/3$. For $x_{Mn} > 1/3$ (ex. $YMnO_3$), 4 J_1 and 2 J_2 are in the plane. For $x_{Mn} < 1/3$ (ex. $LuMnO_3$), 2 J_1 and 4 J_2 are in the plane. The J_1 and J_2 are in-plane exchange interactions and J_1^c and J_2^c are inter-plane exchange interactions. H_{aniso} is the single ion anisotropy term which contains the out-of-plane anisotropy D_1 and the in-plane anisotropy D_2.

$$H_{aniso} = D_1 \sum_i (\mathbf{S}_i^z)^2 + D_2 \sum_i (\mathbf{S}_i \cdot \mathbf{n}_i)^2 \qquad (2)$$

We focused on the spin wave dispersion at low energy. The intra-plane and inter-plane exchange parameters and anisotropy parameters are determined for both magnetic structures described above. The results are summarized in Table II. At T = 1.5 K in both magnetic structures, the determined parameters are J_1's are about 20 percent stronger than J_2's, while D_1 = 0.300(1) meV and D_2 = -0.0013(1) meV. The measured D_1 is reasonably close to those of $YMnO_3$ and $LuMnO_3$ while D_2 is one order of magnitude less. The $|J_1^c - J_2^c|$ is zero within the error. At T = 35 K, the determined parameters J_1 and J_2 become equal and the D_1 and D_2 stay the same. The $|J_1^c - J_2^c|$ is still zero within the error. Just below the anti-ferromagnetic transition temperature, J_1 and J_2 are still equal but 40 to 50 percent smaller while D_1 increases. These results show that, while neutron powder diffraction has shown no clear trimerization in the position of x_{Mn}, the system trimerizes due to the exchange parameter J_1 being stronger at lower temperatures. In other words, a weak trimerization occurs while cooling the $Lu_{0.3}Y_{0.7}MnO_3$.

(Lu,Y)MnO_3	J_1	J_2	J_1/J_2	J_1^c	J_2^c	D_1	D_2	α	ref
$YMnO_3$	4	1.8	2.22	-	-	0.28	-0.02	-	[12]
$YMnO_3$	2.5	2.5	1	-	-	0.28	-0.02	16	[12]
$YMnO_3$	3.4(2)	2.02(7)	1.68	0.014(2)	0	0.28(1)	-0.0007(6)	-	[5]
$YMnO_3$	2.43	2.43	1	0.00015	0.0026	0.32	-	-	[8]
$YMnO_3$	2.4	2.4	1	-	-	0.31	0.036*	-	[6]
$Lu_{0.3}Y_{0.7}MnO_3$	2.65(5)	2.32(5)	1.14	0	0.0012(4)	0.44(1)	0	-	[10]
$Lu_{0.5}Y_{0.5}MnO_3$	12.5	0.97	12.9	-	-	0.28	-0.02	-	[12]
$Lu_{0.5}Y_{0.5}MnO_3$	2.7	2.7	1	-	-	0.28	-0.02	20	[12]
$LuMnO_3$	9	1.4	6.43	-0.018	0	0.28	-0.006	-	[12]
$LuMnO_3$	3	3	1	-	-	0.28	-0.02	16	[12]
$LuMnO_3$	4.09(2)	1.54(5)	2.66	0	0.019(2)	0.48	-	-	[9]
$LuMnO_3$	2.45	2.45	1	$J_1^c - J_2^c =$	0.018	0.48	0.0008	-	[35]
$C_3\Gamma_3 + C_4\Gamma_4$	J_1	J_2	J_1/J_2	J_1^c	J_2^c	D_1	D_2		
$Lu_{0.3}Y_{0.7}MnO_3$	3.24(2)	2.70(1)	1.20	-0.001(9)	-0.001(9)	0.300(1)	-0.0013(1)	this work at $T = 1.5$ K	
$Lu_{0.3}Y_{0.7}MnO_3$	2.91(2)	2.91(1)	1.00	-0.021(8)	-0.021(8)	0.308(1)	-0.0009(1)	this work at $T = 35$ K	
$Lu_{0.3}Y_{0.7}MnO_3$	1.53(3)	1.51(3)	1.01	-0.010(33)	-0.010(33)	0.637(8)	-0.0000(1)	this work at $T = 70$ K	

TABLE II: (*) Chatterji [6] uses a slightly different definition of $D_2 \sum_i (S_i^y)^2$ instead of $D_2 \sum_i (\mathbf{S}_i \cdot \mathbf{n}_i)^2$. The α is dimensionless exchange-striction coefficient defined in the [12].

Temperature dependence of spin gap

By using the linear spin wave theory, Sato and Tian have discussed the analytic form of the gaps from each branch[5, 10]. There are four branches $\Delta_{11}, \Delta_{12}, \Delta_2$ and Δ_3. Tian *et al.* explains that the smaller gap of Δ_{12} is due to smaller $J_1 - J_2$ and $|J_1^c - J_2^c|$ which corresponding to weak trimerization of the Mn lattice. The gap of Δ_{11} and Δ_{12} should be proportional to $2S\sqrt{-D_2\lambda_1}$ and $2S\sqrt{-D_2\lambda_1 - 2(J_1^c - J_2^c)\lambda_1}$ respectively, with $\lambda_1 = D_1 + \frac{3}{2}J_1 + 2J_2$ as described in previous reports [5, 10]. Here, our observations showed that $|J_1^c - J_2^c| = 0$ thus Δ_{11} and Δ_{12} are degenerate so we can simplify this and solely refer to Δ_1.

The temperature dependence of the gap of Δ_1 at the Γ point of the magnon dispersion was investigated. The magnetic excitation from the single crystal data shows the spin gap gradually closes but the changes are rather small. The gap of $\Delta_1 \sim 0.5$ meV close to the transition temperature (shown in Figure 4).

The gap, Δ_1, of $Lu_{0.3}Y_{0.7}MnO_3$ is about five times weaker compared to that of $YMnO_3$ and $LuMnO_3$. The J_1, J_2, and D_1 are similar to those of the previously reported compounds while D_2 is one order of magnitude less. Here D_2 is the in-plane anisotropy.

The energy of Δ_2 and Δ_3 reduce and the dispersion flattens as temperature increases as shown in Figure 3. If we defined the parameter $\lambda_1 = D_1 + \frac{3}{2}J_1 + 2J_2$, this is shown to decrease by about 40 percent between 70K and 1.5 K. The decreasing gap with increasing temperature could be partially attributed to the change of J_1 and J_2 in the Mn triangular plane, however, this is not the sole source of temperature dependence. The D_2 can also contribute to the temperature dependence as $\Delta_1 = 2S\sqrt{-D_2\lambda_1}$ with $\lambda_1 = D_1 + \frac{3}{2}J_1 + 2J_2$. Unfortunately, the contributions from D_1 and D_2 to the change in Δ_1 are too small to detect from this measurement.

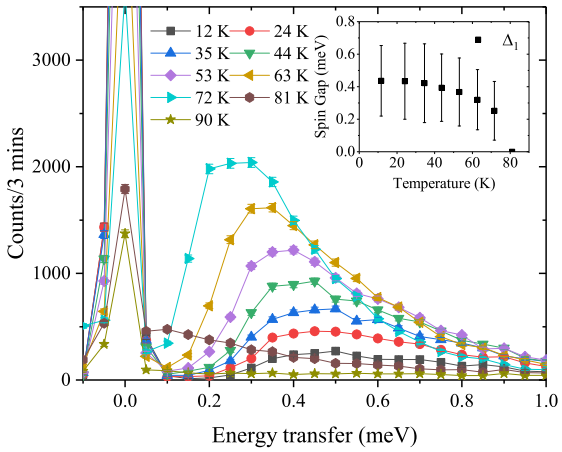

FIG. 4: The temperature dependence of Δ_1 gap at the Γ point

Extended critical scattering range in $Lu_yY_{1-y}MnO_3$

The trimerization could involve many atoms in the unit cell of $Lu_{0.3}Y_{0.7}MnO_3$ while the magnetic excitation tells us the system is a well-defined 2D triangular Heisenberg

antiferromagnet. The nearest neighbour antiferromagnetic Heisenberg exchange is $J_{1,2} \sim 1.5$ meV at 70K. So, a stronger easy-plane anisotropy within the hexagonal plane with $D_1/J_{1,2} \sim 0.40$ and weaker inter-layer interactions with $J^c_{1,2}/J_{1,2} \sim 0.007$ which is one order smaller even compared to $LuMnO_3$ and $YMnO_3$. As revealed by the small Δ_1 gap observed in $Lu_{0.3}Y_{0.7}MnO_3$ including previous results[5, 10], these inter layer interactions are weak. The system cannot break the triangular symmetry, so two-dimensional spin fluctuations should remain.

We observed gap-less magnetic excitations both above and below the ordering temperatures on powder measurements obtained using the Pelican time-of-flight spectrometer for samples with $y = 0.15$, 0.30, and 0.45. These excitations are observed in the Q range ~ 1.28, 2.44 Å^{-1} and energy transfer from 0 to 6.0 meV above T_N and persist up to about 3 T_N as shown in Figure 5 and 6. These $Q = 1.28$ and 2.44 Å^{-1} are corresponding to the (100) = 1.19 Å^{-1} or (101) = 1.31 Å^{-1} and the (200) = 2.38 Å^{-1} or (201) = 2.44 Å^{-1}. Although the excitation we observed is powder averaged, the FWHMs of the excitation has a peak at 150 K of 0.6 Å^{-1} but still remain significant up to ~ 3 T_N as shown in Figure 7.

Such excitations are commonly observed in $LuMnO_3$ [19], $YMnO_3$ [5, 17], ScMnO3 [37], and other 2D-THAs. It's possible that this spectroscopic signature could be a universal phenomenon in the development of spin correlations in 2D-THAs. Further systematic investigations with single crystal samples of 2D-THAs are needed. The $Lu_{0.3}Y_{0.7}MnO_3$ is more suitable because the interlayer interaction and trimerization of $Lu_{0.3}Y_{0.7}MnO_3$ are weaker than that of $YMnO_3$.

Discussion

The crystal and magnetic structural analyses of these $Lu_yY_{1-y}MnO_3$ ($y = 0.15$, 0.30, and 0.45) show that trimerization of this compound is not manifested in the Mn-Mn distance. The magnetic structure continuously adjusts while cooling for all three compounds and can be explained by a linear combination of the irreducible representations Γ_3 and Γ_4. In this case of $Lu_yY_{1-y}MnO_3$, the system favours Γ_3 over Γ_4. There is no clear cross over $x_{Mn} = 1/3$, however, the magnetic structure gets more of Γ_3 by cooling the system while the change of x_{Mn} is not obvious. The linear combinations of Γ_3 ($P6'_3cm'$) and Γ_4 ($P6'_3c'm$) can form the magnetic structure Γ_6 ($P6'_3$), the only way to distinguish these two magnetic structures Γ_5 ($P6_3$) and Γ_6 ($P6'_3$) would be to employ polarized neutron scattering experiment on $Lu_{0.3}Y_{0.7}MnO_3$ and this is planned for subsequent work. So far, the Γ_6 ($P6'_3$) $= C_3\Gamma_3 + C_4\Gamma_4$ was preferred because of the absence of a magneto-elastic coupling in $YMnO_3$ as discussed by some authors [16, 39]. An interesting difference is while the Γ_5 ($P6_3$) admits weak ferromagnetism along the c-axis while the Γ_6 ($P6'_3$) does not. This could be important evidence to determine the magnetic structure of 2D-THA uniquely.

The spin wave dispersion measurements focused on the low energy range and allowed us to determine the exchange interactions of $Lu_{0.3}Y_{0.7}MnO_3$. Just below the transition temperature, J_1 and J_2 are equal. At lower temperatures, J_1 and J_2 differ by 20 percent, on the other hand $D_1 \sim 0.3$ meV and the $|J^c_1 - J^c_2|$ are zero within our resolution. The parameter D_1 are about 0.3 meV at 1.5 K and 30 K which is consistent with previous studies. The parameter D_2 is of the order of μeV or less for all temperatures we measure. From the crystal structural analysis, the trimerization of Mn-Mn was not observed as the x_{Mn} position almost is constant, while the temperature dependence of the exchange parameters supported the weak trimerization of exchange parameters in the plane, so can be described as super-exchange type as suggested [13]. The determined exchange parameters suggested that we captured how the frustrated magnetic system releases the frustration by trimerizing the triangular lattice through the magneto-elastic coupling however the change is not dramatic as in $YMnO_3$, $Lu_{0.5}Y_{0.5}MnO_3$ or $LuMnO_3$ so it is weak at $Lu_{0.3}Y_{0.7}MnO_3$. The Δ_1 gap is about five times smaller compared to $YMnO_3$ and $LuMnO_3$. Since the order of $J_1 = J_2$, and D_1 are the same and $|J^c_1 - J^c_2|$ is within zero, the $\Delta_{11} = \Delta_{12} = \Delta_1 = 2S\sqrt{-D_2\lambda_1}$ with $\lambda_1 = D_1 + \frac{3}{2}J_1 + 2J_2$. These J_1, J_2, and D_2 would be the main contributors to the size of the gap and its temperature dependence. Since by cooling $Lu_yY_{1-y}MnO_3$, the population of Γ_3 increase so that they are more stable under the trimerized state with $J_1 > J_2$.

These determined exchange parameters above suggested the inter plane interaction is weaker so the 2D spin fluctuation also exists on the $Lu_yY_{1-y}MnO_3$. The diffusive inelastic or elastic scatterings that persisted above ordering temperature are abundant in 2D-THAs. Other than $RMnO_3$, the robust spin cluster contrast with conventional magnetic ordering observed for $CuCrO_2$ with triangular lattice Heisenberg antiferromagnets [20]. Other spin order by frustration in triangular lattice Mott insulator $NaCrO_2$, there is a cooperative paramagnetic continuum centered at $Q = 1.4$ Å^{-1} due to fluctuations of small 120° -type clusters above T_N [40]. The Ag_2CrO_2 show the similar feature [41] Similar observations are not limited to the 2D-THAs. For examples, spin dynamics in the pyrochlore antiferromagnet $Y_2Mo_2O_7$ [42], the zigzag chain compound $SrCuO_2$ [43], a geometrically frustrated antiferromagnet $ZnCr_2O_4$ [24, 38], ZnV_2O_4 [23], a triangular antiferromagnet $La_2Ca_2MnO_7$ [44], another geometrically frustrated Spinel $MgCr_2O_4$ all showed magnetic fluctuation above their T_Ns.

However, there is no systematic study performed yet. As suggested by [29], a new classification of these spin liquid-like magnetic excitation above magnetic transition temperatures is needed. Although our results are pow-

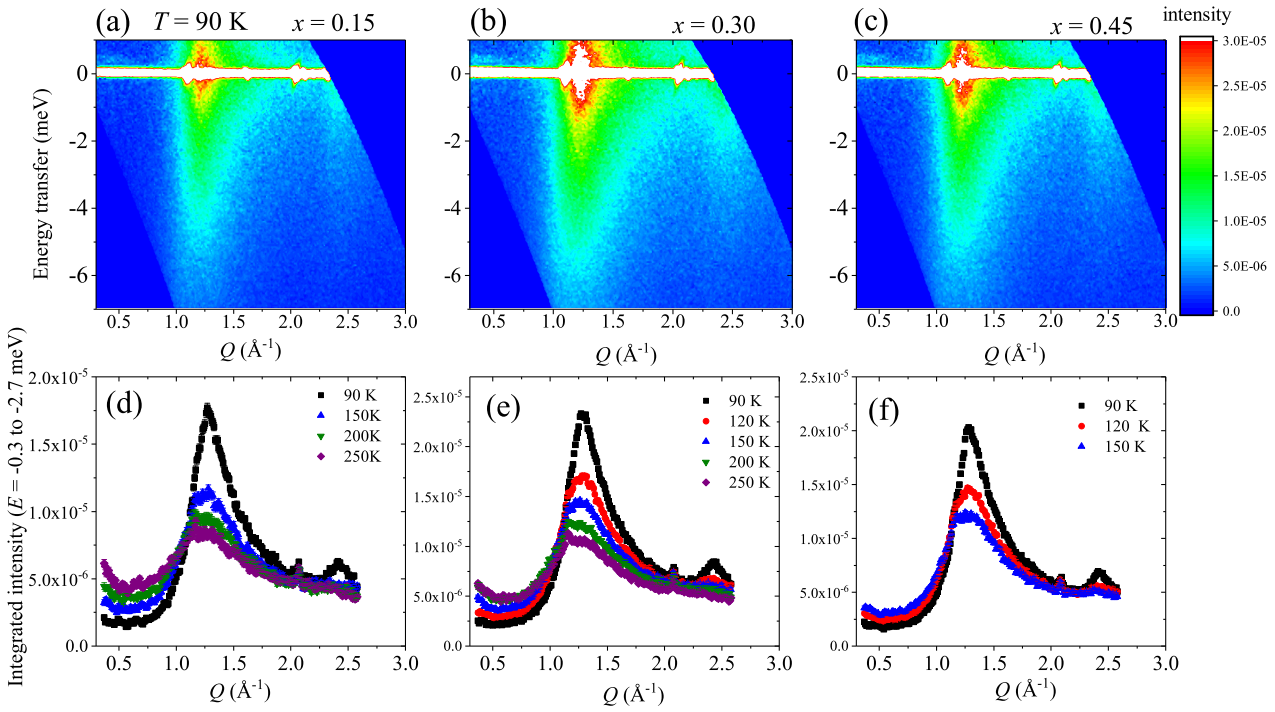

FIG. 5: The observed diffusive inelastic scattering at $x = 0.15$, 0.30, and 0.45. 2nd line) The scattering intensity integrated energy transfer from -0.3 to 2.7 meV.

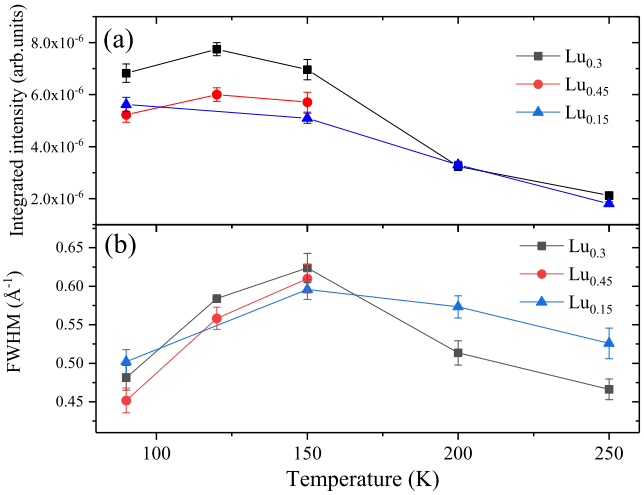

FIG. 6: (q) The temperature dependence of integrated intensities of diffusive inelastic scattering observed at PELICAN. (b) The temperature dependence of FWHM of diffusive inelastic scattering observed at PELICAN.

der averaged, the integrated intensities of diffusive scattering gradually decrease with increasing temperature. The integrated intensity has a maximum at $T \sim 120$ K just above transition temperatures of $T_N \sim 80$ K. The FWHM does not diverge up to 3 T_N. The weaker inter layer interaction supports the argument that the diffuse scattering is from two-dimensional magnetic frustration. The diffusive excitations observed for $Lu_yY_{1-y}MnO_3$ also show critical spin fluctuation existing in a vastly extended critical region observed like $YMnO_3$ [29]. Since the weaker inter-layer interactions with $J^c_{1,2}/J_{1,2} \sim 0.007$ which is one order smaller even compared to $LuMnO_3$ and $YMnO_3$ and there exist only a weak trimerization, the $Lu_{0.3}Y_{0.7}MnO_3$ is a more suitable sample to investigate this phenomena. The study of the single crystal $Lu_{0.3}Y_{0.7}MnO_3$ needs to be performed.

Summary

The detailed investigation of $Lu_yY_{1-y}MnO_3$ has been performed. Structural analyses show no obvious trimerization happens at x_{Mn} position of the composition of $y = 0.15$, 0.30 and 0.45. The results showed the magnetic structure of $Lu_yY_{1-y}MnO_3$ can be described by linear combinations of Γ_3 and Γ_4 and the fraction of Γ_3 kept growing while cooling, so the ground state of the $Lu_yY_{1-y}MnO_3$ favour Γ_3 over Γ_4. The Lu substitutions increase the fraction of Γ_4. The spin wave at low energy and linear spin wave theory captured a weak trimerization on the nearest neighbour exchange coupling

of Mn-Mn (J_1) is happening gradually enhanced while cooling the system. The spin gap Δ_1 of $Lu_{0.3}Y_{0.7}MnO_3$ is about five times smaller compared to that of $LuMnO_3$ and $YMnO_3$ because of in-plane anisotropy D_2 is one order smaller while J_1, J_2, and D_1 are same order. That gap also has temperature dependence which is mainly attributed to the change of J_1, J_2 and D_2. The inter layer couplings are weak, the 2D dimensional fluctuation shows diffusive behaviour above T_N that could be critical spin fluctuation in an extended critical region like on the 2D-THA and other frustrated magnets. Our results showed the single crystal of $Lu_{0.3}Y_{0.7}MnO_3$ could be a suitable candidate to investigate the fluctuation.

ACKNOWLEDGEMENT

Financial supports of the neutron scattering instrument SIKA are from the Ministry of Science and Technology, Taiwan (grant numbers MOST 109-2739-M-213-001) are gratefully acknowledged. SY is financially supported by the National Science and Technology Council, Taiwan, with grant numbers MOST 110-2112-M-213-013 and 111-2112-M-213-023. WC is partially supported by the National Science and Technology Council, Taiwan, with grant no. 110-2124-M-002-019. DL is supported by the Department of Energy (DOE), Grant number DE-FG02-01ER45927. The experiments were performed under ANSTO user program. The proposal numbers are PELICAN (P4341) and SIKA (P7830).

REFERENCES

[1] H. L. Yakel Jnr, W. C. Koehler, E. F. Bertaut and E. F. Forrat, Acta Cryst. **16**, 957-962 (1963).
[2] I.V. Solovyev, M.V. Valentyuk, V.V. Mazurenko, Phys. Rev. B **86** 054407 (2012).
[3] Junghwan Park, Seongsu Lee, Misun Kang, Kwang-Hyun Jan, Changhee Lee, S. V. Streltsov, V.V. Mazurenko, M.V. Valentyuk, J.E. Madevedeva, T. Kamiyama and J. -G. Park, Phys. Rev. B **82**, 054428 (2010).
[4] P. Tong, D. Louca, N. Lee, S.-W. Cheong, Phys. Rev. B **86**, 094419 (2012).
[5] T. J. Sato, S. -H. Lee, T. Katsufuji, M. Masaki, S. Park, J. R. D. Copley, and H. Takagi, Phys. Rev. B **68**, 014432 (2003).
[6] Tapan Chatterji, S. Ghosh, A. Singh, L. P. Regnault, and M. Rheinstädter Phys. Rev. B **76**, 144406 (2007)
[7] Tapam Carrterji, Paramana J. Phys. **71**, 847 (2008).
[8] S. L. Holm, A. Kreisel, T. K. Schäffer, A. Bakke, M. Bertelsen, U. B. Hansen, M. Retuerto, J. Larsen, D. Prabhakaran, P. P. Deen, Z. Yamani, J. O. Birk, U. Stuhr, Ch. Niedermayer, A. L. Fennell, B. M. Andersen, and K. Lefmann, Phys. Rev. B **97**, 134304 (2018)
[9] H. J. Lewtas, A. T. Boothroyd, M. Rotter, D. Prabhakaran, H. Müller, M. D. Le, B. Roessli, J. Gavilano, and P. Bourges, Phys. Rev. B **82**, 184420 (2010).
[10] W. Tian, Guotai Tan, Liu Liu, Jinxing Zhang, Berry Winn, Tao Hong, J.A. Fernandez-Baca, Chenglin Zhang, Pengcheng Dai, Phys. Rev. B **89** 144417 (2014).
[11] J.Oh, Manh Duc Le, J. Jeong, J. Lee, H. Woo, W-Y Song, T.G. Perring, W.J.L. Buyers, S.-W. Cheong, and Je-Geun Park, Phys. Rev. Lett. **111** 257202 (2013).
[12] J.Oh, Manh Duc Le, Ho-Hyun Nahm, Hasung Sim, Jaehong Jeong, T.G. Perring, Hyungje Woo, Kenji Nakajima, Seiko Ohira-Kawamura, Zahra Yamani, Y. Yoshida, H. Eisaki, S.-W. Cheong, A.L.Chernyshev and Je-Geun Park, Nat. Commun. **7** 13146 (2016).
[13] Kisoo Park, Joosung Oh, Ki Hoon Lee, Jonathan C. Leiner, Hasung Sim, Ho-Hyun Nahm, Taehun Kim, Jaehong Jeong, Daisuke Ishikawa, Alfred Q. R. Baron, and Je-Geun Park, Phys. Rev. B **102**, 085110 (2020)
[14] X. Fabrèges, S. Petit, I. Mirebeau, S. Pailhès, L. Pinsard, A. Forget, M. T. Fernandez-Diaz, and F. Porcher, Spin-Lattice Coupling, Phys. Rev. Lett. **103**, 067204 (2009).
[15] M. Fiebig, D. Fröhlich, K. Kohn, St. Leute, Th. Lottermoser, V. V. Pavlov, and R. V. Pisarev, Phys. Rev. Lett. **84**, 5620 (2000)
[16] P J Brown and T Chatterji, J. Phys. Condens. Matter **18**, 10085-10096 (2006).
[17] Junghwan Park, J.-G. Park, Gun Sang Jeon, Han-Yong Choi, Changhee Lee, W. Jo, R. Bewley, K. A. McEwen, and T. G. Perring, Phys. Rev. B **68**, 104426 (2003),
[18] B. Roessli, S. N. Gvasaliya, E. Pomjakushina, and K. Conder; JETP Letters, Vol. 81, No. 6, pp. 287–291 (2005).
[19] Shin-ichiro Yano, Despina Louca, Songxue Chi, Masaaki Matsuda, Yiming Qiu, John R. D. Copley, and Sang-Wook Cheong, J. Phys. Soc. Jpn. **83** 024601 (2014).
[20] Ryoichi Kajimoto, Keisuke Tomiyasu, Kenji Nakajima, Seiko Ohira-Kawamura, Yasuhiro Inamura, and Tetsuji Okuda, J. Phys. Soc. Jpn. **84**, 074708 (2015)
[21] Junjie Yang, Chunruo Duan, John R. D. Copley, Craig M. Brown and Despina Louca, MRS Advances , Volume 1 , Issue 9: Electronics and Photonics, pp. 565 – 571 (2016).
[22] Steven M. Disseler, Xuan Luo, Bin Gao, Yoon Seok Oh, Rongwei Hu, Yazhong Wang, Dylan Quintana, Alexander Zhang, Qingzhen Huang, June Lau, Rick Paul, Jeffrey W. Lynn, Sang-Wook Cheong, and William Ratcliff, II Phys. Rev. B **92**, 054435 (2015).
[23] S.-H. Lee, D. Louca, H. Ueda, S. Park, T. J. Sato, M. Isobe, Y. Ueda, S. Rosenkranz, P. Zschack, J. Íñiguez, Y. Qiu, and R. Osborn Phys. Rev. Lett. **93**, 156407 (2004).
[24] S.-H. Lee, C. Broholm, T. H. Kim, W. Ratcliff, II, and S-W. Cheong Phys. Rev. Lett. **84**, 3718 (2000).
[25] X. Bai, J. A. M. Paddison, E. Kapit, S. M. Koohpayeh, J. J. Wen, S. E. Dutton, A. T. Savici, A. I. Kolesnikov, G. E. Granroth, C. L. Broholm, J. T. Chalker, and M. Mourigal, Phys. Rev. Lett. **122**, 097201 (2019).
[26] T. H. Han, J. S. Helton, S. Chu, D. G. Nocera, J. A. Rodriguez-Rivera, C. Broholm, and Y. S. Lee, Fractionalized excitations in the spin-liquid state of a kagome-lattice antiferromagnet, Nature (London) **492**, 406 (2012).
[27] Y. Shen, Y. D. Li, H. Wo, Y. Li, S. Shen, B. Pan, Q. Wang, H. C. Walker, P. Steffens, M. Boehm, Y. Hao, D.

L. Quintero-Castro, L. W. Harriger, M. D. Frontzek, L. Hao, S. Meng, Q. Zhang, G. Chen, and J. Zhao, Evidence for a spinon Fermi surface in a triangular-lattice quantum-spin-liquid candidate, Nature (London) **540**, 559 (2016).

[28] Kazuki Iida, Hiroyuki Yoshida, Hirotaka Okabe, Naoyuki Katayama, Yuto Ishii, Akihiro Koda, Yasuhiro Inamura, Naoki Murai, Motoyuki Ishikado, Ryosuke Kadono, and Ryoichi Kajimoto, Scientific Reports **9**, 1826 (2019).

[29] Sofie Janas, Jakob Lass, Ana-Elena Ţuţueanu, Morten L. Haubro, Christof Niedermayer, Uwe Stuhr, Guangyong Xu, Dharmalingam Prabhakaran, Pascale P. Deen, Sonja Holm-Dahlin, and Kim Lefmann, Phys. Rev. Lett. **126**, 107203 (2021).

[30] A.J. Studer, M.E. Hagen, T.J. Noakes; Phys. B Condens. Matter 385–386 (2006) 1013–1015.

[31] C.-M. Wu, G. Deng, J.S. Gardner, P. Vorderwisch, W.-H. Li, S. Yano, J.-C. Peng and E. Imamovic; JINST **11** P10009 (2016).

[32] D. H. Yu, R. A. Mole, T. Noakes, S. J. Kennedy and R. A. Robinson, J. Phys. Soc. Jpn. **82** SA027 (2013).

[33] Seongsu Lee, A. Pirogov, Misun Kang, Kwang-Hyun Jang, M. Yonemura, T.Kamiyama, S.-W,Cheong, F.Gozzo, Mamsoo, SHih, H.Kimura, Y.Noda, and J.-G.Park, Nature **451** 805 (2008) .

[34] T. Katsufuji, M. Masaki, A. Machida, M. Moritomo, K. Kato, E. Nishibori, M. Takata, M. Sakata, K. Ohoyama, K. Kitazawa, and H. Takagi, Phys. Rev. B **66**, 134434 (2002).

[35] C. Toulouse, J. Liu, Y. Gallais, M.-A. Measson, A. Sacuto, M. Cazayous, L. Chaix, V. Simonet, S. de Brion, L. Pinsard-Godart, F. Willaert, J. B. Brubach, P. Roy, and S. Petit, Phys. Rev. B **89** 094415 (2014).

[36] S. Petit, F. Moussa, M. Hennion, S. Pailhe‘s, L. Pinsard-Gaudart, and A. Ivanov, Phys. Rev. Lett. **99** 266604 (2007).

[37] M. Bieringer and J. E. Greedan, J. Solid State Chem. **143**, 132 (1999).

[38] W. Ratcliff, II, S.-H. Lee, C. Broholm, S.-W. Cheong, and Q. Huang, Phys. Rev. B **65**, 220406(R) (2002).

[39] Christopher J Howard, Branton J Campbell, Harold T Stokes, Michael A Carpenter, Richard I Thomson; Acta Crystallogr B Struct. Sci. Cryst. Eng. Mater.; **69**, 534-540 (2013).

[40] D. Hsieh, D. Qian, R.F. Berger, C. Liu, B. Ueland, P. Schiffer, Q. Huang, R.J. Cava, J.W. Lynn, M.Z. Hasan, arXiv:1405.6184v1. D. Hsieh, D. Qian, R.F. Berger, R.J. Cava, J.W. Lynn, Q. Huang, M.Z. Hasan, Journal of Physics and Chemistry of Solids **69**, 3174–3175 (2008).

[41] Masaaki Matsuda, Sachith E. Dissanayake, Hiroyuki K. Yoshida, Masaaki Isobe, and Matthew B. Stone, Phys. Rev. B **102**, 214411 (2020).

[42] J. S. Gardner, B. D. Gaulin, S.-H. Lee, C. Broholm, N. P. Raju, and J. E. Greedan, Phys. Rev. Lett. **83**, 211 (1999).

[43] I. A. Zaliznyak, C. Broholm, M. Kibune, M. Nohara, and H. Takagi, Phys. Rev. Lett. **83**, 5370 (1999).

[44] Wei Bao, Y.X. Wang, Y. Qiu, K. Li, J.H. Lin, J.R.D. Copley, R.W. Erwin, B.S. Dennis, A.P. Ramirez, arXiv:0910.1904v1.